



# Rapid synthesis of single-crystalline TbF<sub>3</sub> with novel nanostructure via ultrasound irradiation

Ling Zhu, Yangjia Liu, Xizhi Fan, Daowu Yang, Xueqiang Cao \*

School of Chemical and Biological Engineering, Changsha University of Science and Technology, Changsha 410114, Hunan, China

## ARTICLE INFO

### Article history:

Received 4 July 2010

Received in revised form 29 September 2010

Accepted 1 November 2010

Available online 4 November 2010

### Keywords:

A. Optical materials

A. Nanostructures

C. Ultrasonic measurements

D. Luminescence

## ABSTRACT

Terbium fluoride (TbF<sub>3</sub>) nanopeanut has been successfully synthesized via a mild sonochemical route from an aqueous solution of terbium nitrate and fluoroborate without any template or organic additive. X-ray diffraction, scanning electron microscopy, transmission electron microscopy, and photoluminescence (PL) spectra were utilized to characterize the synthesized samples. The morphologies and optical properties of the obtained TbF<sub>3</sub> nanopeanut can be tuned by ultrasound irradiation as well as the fluoride source. The prepared TbF<sub>3</sub> nanopeanut shows extraordinarily high room temperature photoluminescence intensity comparing to the products prepared by stirring. The possible formation mechanism is proposed in this paper.

© 2010 Elsevier Ltd. All rights reserved.

## 1. Introduction

Over the past decades, many methods have been explored to produce various nanomaterials, such as precipitation, reverse micelles or microemulsions, sol–gel method, electrochemical method, solvothermal route, microwave method, and sonochemical method, etc. Among these methods, sonochemical synthesis has been paid more extensive attention due to its special potential applications. Currently, the sonochemical method has been proven to be an effective approach for generating materials with unusual properties, since it results in particles with a much smaller size and high surface area than those synthesized by other methods [1]. The chemical effect of ultrasonic irradiation arises from the acoustic cavitation, in other words, the formation, growth and implosive collapse of bubbles in the liquid medium. The implosive collapse of the bubbles generates the local hot spots through the shock wave formation within the gas phase of the collapsing bubble. These local hot spots have been shown to be about 5000 K with a pressure of 1800 atm and cooling rate higher than  $10^8 \text{ K s}^{-1}$  [2,3]. The extremely transient high pressure and temperature provide a unique environment for the growth of materials with novel structures. The advantages of this method include a rapid reaction rate, the controllable reaction condition and the ability to form materials with uniform shape, narrow size distribution and high purity. Up to now, nanomaterials with various shapes and structures, such as nanotubes [4,5], nanowires [6,7], nanorods [8,9], hollowed

spheres [10,11], core/shell particles [12,13], have been successfully prepared by this method.

More recently, rare earth fluorides have been attracting much attention due to their unique physical and chemical properties and potential applications in the fields of luminescent, magnets, catalysts, biochemical probes, and so on [14–18]. The investigation on the preparation and properties of rare earth fluorides has attracted a great deal of attention. A variety of methods have been employed to fabricate these materials. For example, the fullerene-like lanthanide fluorides, the bundle-like and rod-like YF<sub>3</sub> were synthesized by a hydrothermal process [19–22]; CeF<sub>3</sub> nanoparticles have been prepared using a polyol method [23]. Chen and coworkers have obtained EuF<sub>3</sub> nanocrystals with different morphologies via a stirring method [24,25]. Reverse micelles and microemulsion techniques were also developed by several groups and have been widely used for the preparation of CeF<sub>3</sub> nanoparticles [26,27], and YF<sub>3</sub> nanoparticles with controllable sizes and morphologies [28]. However, to the best of our knowledge, the synthesis of TbF<sub>3</sub> with the peanut-like nanostructure has not yet been reported. Accordingly, in this paper, we report a facile ultrasonic approach of preparing well-defined TbF<sub>3</sub> nanopeanuts at room temperature without any surfactant or template. It is shown that the sonochemical method is a very powerful approach to synthesize inorganic materials with interesting morphologies.

## 2. Experimental

### 2.1. Synthesis

All the chemicals were of analytical grade and were used as received. In a typical synthesis, an appropriate amount of Tb<sub>4</sub>O<sub>7</sub>

\* Corresponding author. Fax: +86 431 85262285.

E-mail address: [xcao@ciac.jl.cn](mailto:xcao@ciac.jl.cn) (X. Cao).

was first dissolved in 10% nitric acid, and then mixed with the solution of  $\text{KBF}_4$ . The final concentration of  $\text{Tb}(\text{NO}_3)_3$  and  $\text{KBF}_4$  was 30 mM and 60 mM, respectively. The resulted solution was sonicated at ambient temperature for 3 h by a high-intensity ultrasonic probe (JCS-206 Jining Co., China, Ti-horn, 23 kHz). During the sonication, the temperature of the suspension rose to about 70 °C. A white precipitate was centrifuged, washed with distilled water and absolute ethanol in sequence. The final product was dried under vacuum at 60 °C for 12 h. For comparison, a sample of  $\text{TbF}_3$  product was also synthesized via vigorous stirring under the same conditions but without the ultrasonic irradiation. After vigorous stirring for 3 h, the reaction solution was still clear to naked eyes, and no product was formed. Then, the reaction system was kept still for 24 h at room temperature, resulting in the formation of white precipitate.

## 2.2. Characterization

The X-ray powder diffraction (XRD) pattern was performed on a Rigaku D/MAX-2500 diffractometer with  $\text{Cu K}\alpha$  radiation ( $\lambda = 0.15406 \text{ nm}$ ) and a scanning rate of  $5^\circ \text{ min}^{-1}$ . The operation voltage and current were maintained at 40 kV and 200 mA, respectively. Scanning electron micrographs (SEM) images were taken on a XL-30 field-emission scanning electron microscope (Philips) equipped with energy-dispersive X-ray fluorescence analysis (EDXA). Samples for SEM observation were prepared by dropping a diluted suspension of the sample powders on the silicon substrate. Transmission electron microscopy (TEM), selected area electron diffraction (SAED) were recorded on a JEOL-JEM-2010 operating at 200 kV (JEOL, Japan). Samples for TEM observation were prepared by dropping a diluted suspension of the sample powders onto a standard carbon-coated Formvar film (20–30 nm) on a copper grid (230 mesh). Photoluminescence (PL) spectra were recorded with a Hitachi F-4500 spectrophotometer equipped with a 150 W Xenon lamp as the excitation source. All the measurements were performed at room temperature.

## 3. Results and discussion

### 3.1. Structure and morphology control of the nanocrystal

The crystal structure of the as-prepared  $\text{TbF}_3$  samples was characterized by XRD. As shown in Fig. 1a, the XRD pattern of the sample prepared through ultrasonic irradiation is consistent well with the orthorhombic  $\text{TbF}_3$  (JCPDS No. 37-1487). The strong and sharp diffraction peaks indicate that the product is well crystal-

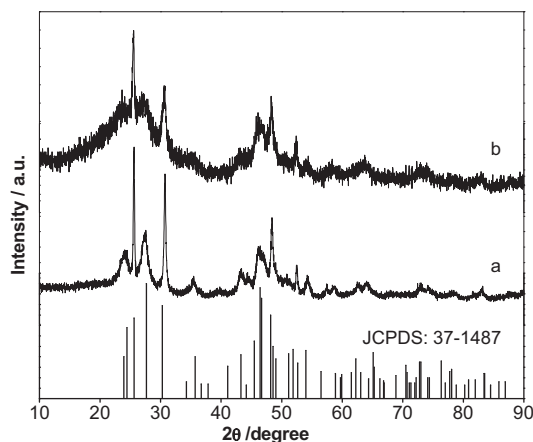


Fig. 1. XRD patterns of  $\text{TbF}_3$  samples prepared with the ultrasonic irradiation (a) and with the mechanic stirring (b).

lized. Furthermore, the sample obtained via stirring shows the similar pattern, indicating the formation of the orthorhombic  $\text{TbF}_3$  crystal (Fig. 1b). While, it is worth noting that the intensity of the diffraction peaks of the product obtained via ultrasonic irradiation are obviously sharper than those of the sample prepared by stirring, as the result of better crystallinity. It has been well documented that the utilization of ultrasonic irradiation in inorganic solution can improve the crystallinity of the products [29–31].

The morphology and microstructure details of the as-prepared  $\text{TbF}_3$  nanocrystals via ultrasound irradiation were investigated by SEM, TEM, and SAED, as shown in Fig. 2. The SEM image with a low magnification (Fig. 2a) reveals that the  $\text{TbF}_3$  sample consists of a large quantity of peanut-like crystals with uniform size. The well-defined peanut-like crystal has good symmetry, with 200 nm in diameter and 550 nm in length as can be seen from the SEM image with a higher magnification (Fig. 2b), and this is confirmed by the TEM observation (Fig. 2e). An enlarged SEM image (Fig. 2c) displays that the surfaces of the peanut-like particles are very scraggy, just like the surface of the peanut. The energy dispersive X-ray spectroscopy analysis (EDXA) confirms that the peanuts are composed of Tb and F in a ratio of about 1:2.9 (Fig. 2d), and gives further support to the XRD analysis as discussed above. The TEM image with a high magnification shows that the peanut-like structures were actually bundles of numerous nanofibers (Fig. 2f), which were about 3 nm wide and 550 nm long. A typical SAED recorded with the electron beam perpendicular to the axis of the  $\text{TbF}_3$  nanopnut is shown in Fig. 2g, showing the single-crystal nature of the sample. The SAED pattern can be indexed as an orthorhombic crystal recorded along the  $[001]$  zone axis. The pattern clearly indicates the orientation alignment among all of the nanofibers in the bundle along  $[010]$ , which shows that the nanowires are aligned not only in length but also in crystallographic orientation. In addition, the SAED pattern shows the symmetrical stripes rather than polycrystalline circles or single-crystal spots, implying the presence of some ordered arrangement of crystallites in the bundle, which is in good agreement with TEM observations. While, the sample which is prepared via vigorous electric stirring instead of the ultrasound irradiation consists of the caddice flowerlike agglomerates as shown in the SEM images of Fig. 3a–c. The individual  $\text{TbF}_3$  flower seems to be composed of the crooked nanorods with diameters ranging from 12 to 20 nm, and each nanorod contains the smaller nanosized particles with sizes ranging from 10 to 20 nm (Fig. 3c).

### 3.2. Effect of fluoroborate

Further experiments indicate that the use of fluoroborate as the fluoride source is one of the key factors to control the morphology of the final product. When  $\text{NaBF}_4$  was used as the fluoride source, the product with a similar morphology (peanut-like) and size was obtained (Fig. 4a) by the identical ultrasonic process. If  $\text{NaF}$  or  $\text{NH}_4\text{F}$  was used as raw materials, and the other experimental conditions were unchanged, only the irregular nanoparticles with serious agglomeration were formed (Fig. 4b and c). Therefore, it is concluded that the fluoroborate has an important effect on the morphology of the as-formed product. On one side, the fluoroborate serves as the source of the fluoride ion. On the other side, during the hydrolysis of  $\text{KBF}_4$  in aqueous solution,  $\text{BO}_3^{3-}$  ions are produced in the reaction solution, as shown in Eq. (1) (discussed later) and have been proved by the other group [32]. It is quite possible that these  $\text{BO}_3^{3-}$  anions are adsorbed on one specific plane of the crystal seed, which result in the formation of the product with anisotropic growth. It is well documented that the adsorbed ions can change the growth kinetics and surface energies of different crystal faces, which can ultimately lead to anisotropic

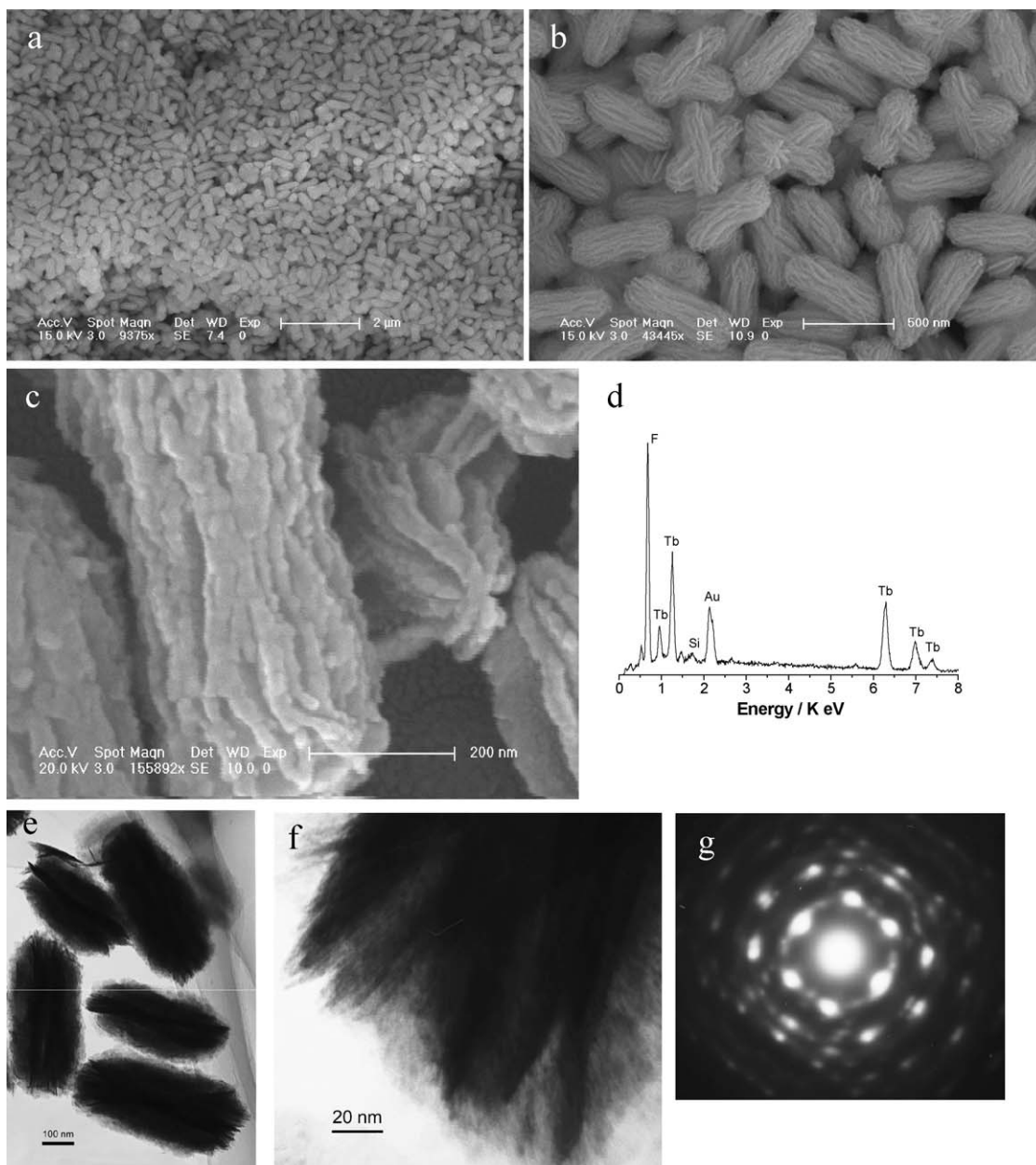


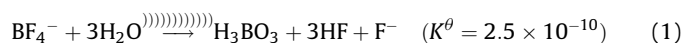
**Fig. 2.** SEM images of the as-prepared  $\text{TbF}_3$  peanuts with different magnifications (a–c), EDX of peanuts (d), TEM image (e), TEM image with large magnification (f), and SEAD of  $\text{TbF}_3$  peanut-like particles (g).

growth of low symmetry nanostructures [33–37]. For example, Pileni and coworkers have demonstrated that the chloride and bromide ions which could be selectively adsorb on the (001) and (111) faces to favor either crystal growth on the [110] direction or to form cubes of copper nanostructures in a micelle system [34]. Liu and coworkers used a seed growth procedure to obtain a complex hexagonal ZnO nanostructure with capping of the citric acid, which adsorbs preferably on the (001) surface of ZnO and slows down the crystal growth along the *c*-axis [36]. Hence, fluoroborate might play a key role in the formation of  $\text{TbF}_3$  nanopanutes in the adopted reaction system.

### 3.3. Effect of ultrasound irradiation and the possible growth mechanism

It has been well established that the ultrasonic irradiation introduces unusual physical and chemical effects deriving from the

acoustic cavitation. Such cavitation behavior leads to many unique properties in the irradiated solution and it has been used extensively to generate materials with interesting morphologies. Therefore, the ultrasound appears to be particularly effective as a means of inducing nucleation and may influence crystallization, which is another key factor for the formation of final peanut-like  $\text{TbF}_3$  product. In aqueous solution  $\text{KBF}_4$  was slowly hydrolyzed to produce  $\text{F}^-$ ; these  $\text{F}^-$  anions react with  $\text{Tb}^{3+}$  cations to form terbium fluoride shown in the following equations.



The equilibrium-constant of the hydrolysis reaction (Eq. (1)) is very small, which will keep the low concentration of  $\text{F}^-$  ions in the reaction solution, and consequently leads to the slow crystalliza-

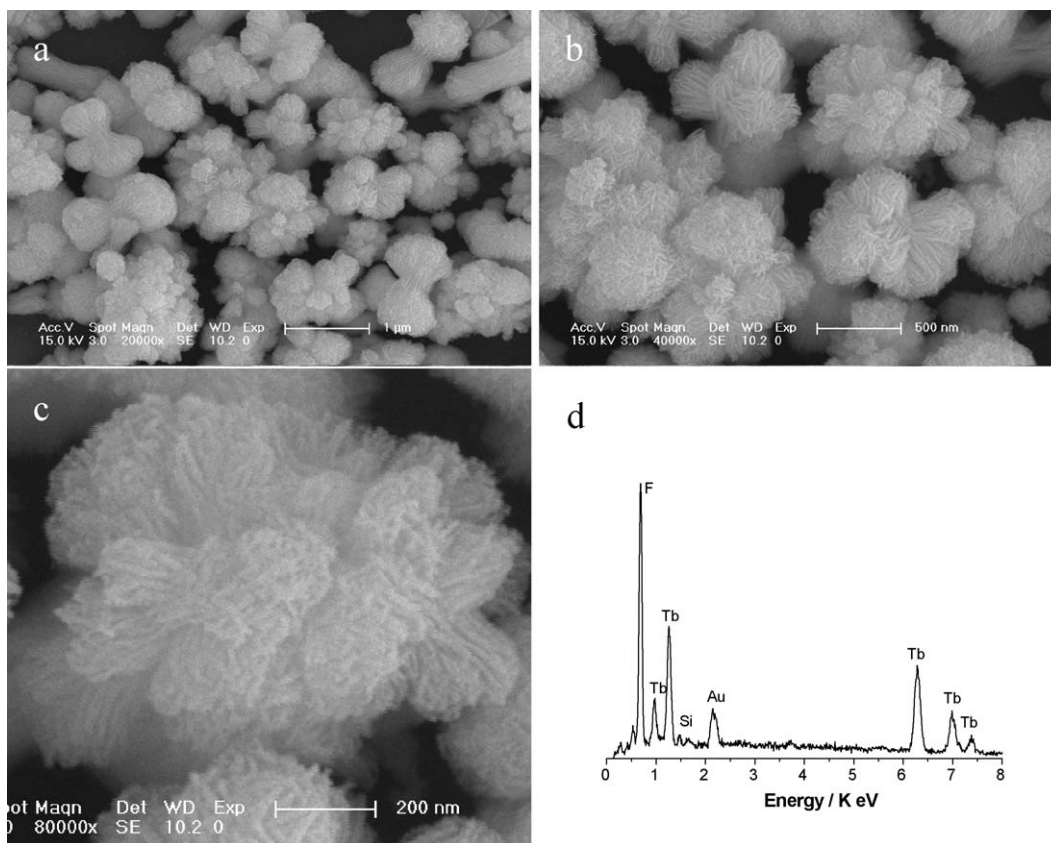


**Fig. 3.** SEM images of the as-prepared  $\text{TbF}_3$  sample with different magnifications prepared via vigorous electric stirring (a–c) and its EDX analysis (d).

tion process. However, the employing of the ultrasonic irradiation will accelerate the hydrolysis process, which is presumably helpful to the nucleation and growth of the  $\text{TbF}_3$  nanocrystals. Furthermore, the cavitation and shock wave created by the ultrasound can accelerate the formation of solid particles to high velocities, which leading to the interparticle collision and effective fusion at the point of collision. With these merits, the fabrication time of nanomaterial under ultrasound irradiation is significantly reduced.

In the case of the stirring method, no product was formed after the vigorous stirring for 3 h. The product of the caddice flowerlike agglomerates was formed after the reaction solution was kept still for 24 h and only a little product was obtained. This result further proves that the hydrolysis process of  $\text{KBF}_4$  is very slow at room temperature. Considering that the  $\text{CaMoO}_4$  and  $\text{SrMoO}_4$  particles with similar shape have been produced by the similar method [38] and it has been disclosed that the mineralization process resulted in the formation of the complicated structures [38]. Therefore, it is possible that the caddice flower-like agglomerate was also formed by the mineralization process of  $\text{TbF}_3$  microcrystallites at room temperature.

To further investigate the details of the formation of  $\text{TbF}_3$  nanopeanuts under ultrasound irradiation, the growth process of the final product was carefully monitored by time-dependent experiments. SEM images with different reaction time show an obvious growth process from the small primary nanoparticles to the final peanuts (Fig. 5). With ultrasonic treatment for 20 min, the transparent reaction solution became turbid, which indicates the formation of nuclei. When reaction up to 30 min, a white precipitate appeared, showing the formation of disk-like particles (Fig. 5a). Furthermore, these disk-like particles would like to further grow in some specific orientations to form peanut-like structures (Fig. 5b and c). Usually, the growth of the peanut-like product will complete in 3 h (Fig. 5d). And it is also observed that the morphology and size of the product have no obviously changed by further prolonging the sonication time. In this work, the ultrasound irradiation played an important role in the formation of the final product. The employing of the ultrasonic irradiation would accelerate the hydrolysis process, and lead to the formation of the small primary nanoparticles. With the ongoing of the

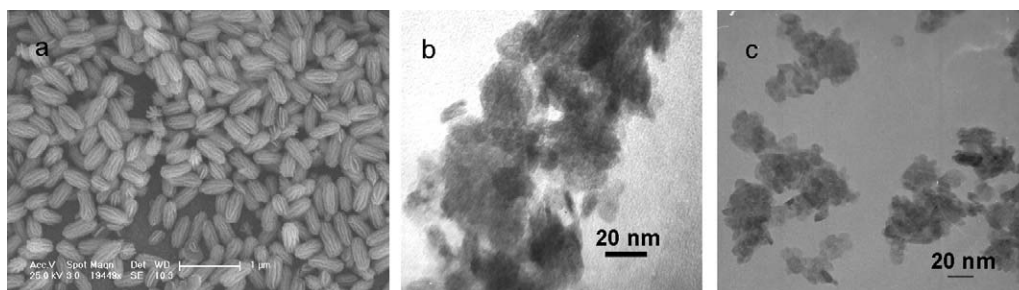


**Fig. 4.** SEM image and TEM images of the as-prepared  $\text{TbF}_3$  sample via ultrasound irradiation with the fluoride source of  $\text{NaBF}_4$  (a),  $\text{NaF}$  (b) and  $\text{NH}_4\text{F}$  (c).

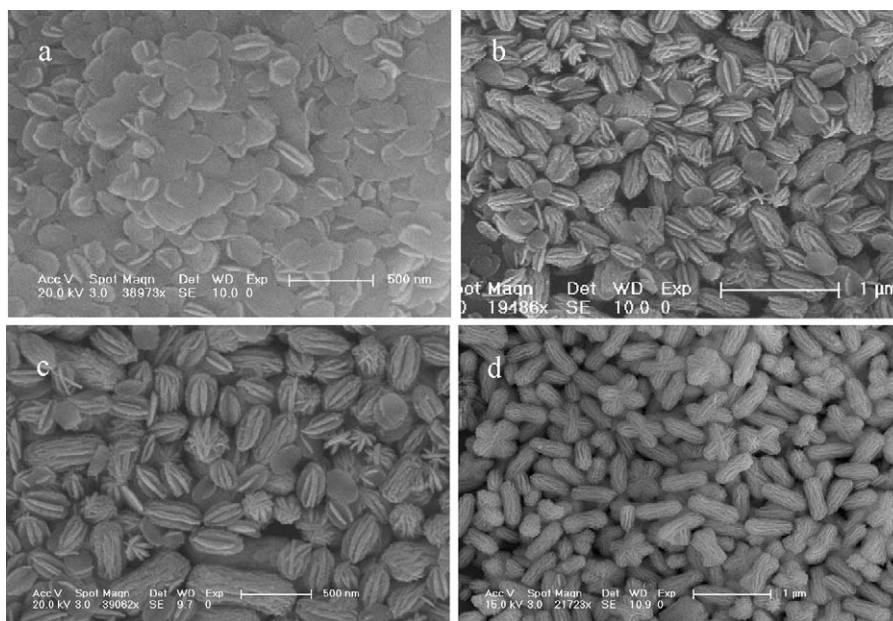


Fig. 5. The time-dependent SEM images of the peanut-like crystals after ultrasound treatment for 0.5 h (a), 1 h (b), 2 h (c) and 3 h (d).

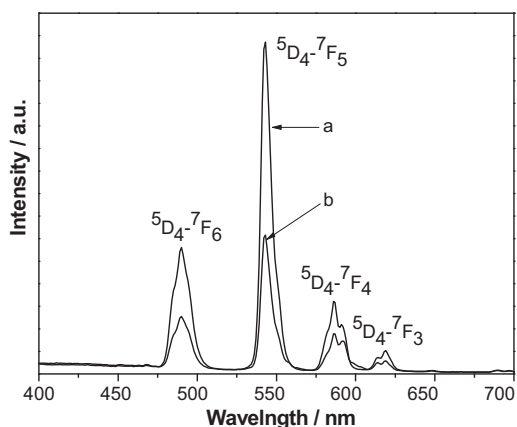


Fig. 6. Room-temperature PL spectra of the as-prepared  $\text{TbF}_3$  peanuts via sonochemical method (a) and the  $\text{TbF}_3$  flowers by vigorous electric stirring (b).

reaction, the primary nanoparticles further grow to the nanodisks, and then the freshly formed nanoparticles will spontaneously “land” on the as-formed disks in some specific orientations to form the peanut-like structure. Although the exact formation mechanism for this complex nanostructure is not yet very clear, it is believed that the growth of the peanut-like nanostructures is not catalyst-assisted or template-directed, because the only material sources used in our synthesis are pure rare earth oxide crystals and fluoroborate. In the present case, the role of sonication is not only to accelerate the reaction between the raw materials but also to lead to the growth and crystallization of  $\text{TbF}_3$  due to its extreme conditions.

### 3.4. Optical property

Fig. 6 shows the room-temperature emission spectra of  $\text{TbF}_3$  products obtained in the presence and absence of ultrasound irradiation. Both the samples were measured under identical conditions with the excitation wavelength  $\lambda_{\text{ex}} = 350 \text{ nm}$ . The emission spectra of these two samples show similar patterns and have a characteristic emission peaks of  $\text{Tb}^{3+}$  within the wavelength

range from 470 to 630 nm, corresponding to the transitions from the excited levels of  $^5\text{D}_4$  to  $^7\text{F}_j$  ( $J = 3-6$ ), with the electronic transition  $^5\text{D}_4 - ^7\text{F}_5$  (543 nm) being the most prominent emission line [39,40]. Furthermore, it is worth noting that the emission intensity of the  $\text{TbF}_3$  nanopeanuts is much higher than that of the flower-like product which was prepared via vigorous stirring. The crystallinity of  $\text{TbF}_3$  nanopeanuts prepared via the ultrasonic irradiation obviously is higher than that of the flower-like  $\text{TbF}_3$  prepared by stirring (as shown in Fig. 1). The high crystallinity favors the improvement of the luminescent intensity of products [41,42]. It is also assumed that the flower-like crystals would possess more defects, and some of these defects may act as the nonradiative recombination centers, which will lead to lower intense emission. These results indicate that the luminescence properties of  $\text{TbF}_3$  are largely affected by factors such as the morphology, the crystallinity, and the structural defects.

## 4. Conclusion

In summary, terbium fluoride with novel nanostructure has been successfully synthesized via a mild sonochemical route. The ultrasonic irradiation as well as the fluoroborate has a remarkable effect on the morphology of the final product. This simple and unique synthetic method has a potential advantage for synthesis of novel materials or materials with novel morphology. Room temperature photoluminescence of  $\text{TbF}_3$  samples formed with the two methods have similar features with the characteristic emission of  $\text{Tb}^{3+}$  transitions, but the emission intensity of the peanut-like  $\text{TbF}_3$  nanocrystals under ultrasound irradiation was greatly improved comparing with the product prepared via stirring.

## Acknowledgements

Financial support from the National Natural Science Foundation of China (21001017), Startup Fund for Doctoral Program, Huxiang Scholars Program and Hunan Provincial Key Laboratory of Materials Protection for Electric Power and Transportation (2011CL02) (Changsha University of Science & Technology) are gratefully acknowledged.

## References

- [1] J. Lu, Y. Xie, X.H. Jiang, W. He, G.A. Du, J. Mater. Chem. 11 (2001) 3281–3284.
- [2] K.S. Suslick, Science 247 (1990) 1439.
- [3] S. Avivi, Y. Mastai, G. Hodes, A. Gedanken, J. Am. Chem. Soc. 121 (1999) 4196.
- [4] R. Katoh, Y. Tasaka, E. Sekreta, M. Yumura, F. Ikazaki, Y. Kakudate, S. Fujiwara, Ultrason. Sonochem. 6 (1999) 185.
- [5] Y.C. Zhu, H.L. Li, Y. Koltypin, Y.R. Hacoheh, A. Gedanken, Chem. Commun. 24 (2001) 2616.
- [6] B. Gates, B. Mayers, A. Grossman, Y.N. Xia, Adv. Mater. 14 (2002) 1749.
- [7] B.T. Mayers, K. Liu, D. Sunderland, Y.N. Xia, Chem. Mater. 15 (2003) 3852.
- [8] H. Wang, J.J. Zhu, J.M. Zhu, H.Y. Chen, J. Phys. Chem. B 106 (2002) 3848.
- [9] L. Zhu, X.M. Liu, X.D. Liu, Q. Li, J.Y. Li, S.Y. Zhang, J. Meng, X.Q. Cao, Nanotechnology 17 (2006) 4217.
- [10] X.W. Zheng, Y. Xie, L.Y. Zhu, X.C. Jiang, A.H. Yan, Ultrason. Sonochem. 9 (2002) 311.
- [11] J.L. Yin, X.F. Qian, J. Yin, M.W. Shi, G.T. Zhou, Mater. Lett. 57 (2003) 3859.
- [12] M.L. Breen, A.D. Dinsmore, R.H. Pink, S.B. Qadri, B.R. Ratna, Langmuir 17 (2001) 903.
- [13] N.A. Dhas, A. Gedanken, Appl. Phys. Lett. 72 (1998) 2514.
- [14] S.J. Zeng, G.Z. Ren, W. Li, C.F. Xu, Q.B. Yang, J. Phys. Chem. C 114 (2010) 10750–10754.
- [15] P. Belli, R. Bernabei, R. Cerulli, C.J. Dai, F.A. Danevich, A. Incicchitti, V.V. Kobychev, O.A. Ponkratenko, D. Prospero, V.I. Tretyak, Y.G. Zdesenko, Nucl. Instrum. Methods A 498 (2003) 352.
- [16] M.L. Paradowski, A.W. Pacyna, A. Bombik, W. Korczak, S.Z. Korczak, J. Magn. Magn. Mater. 212 (2000) 381.
- [17] J.Z. Luo, H.L. Wan, Appl. Catal. A: Gen. 158 (1997) 137.
- [18] L.Q. Xiong, Z.G. Chen, M.X. Yu, F.Y. Li, C. Liu, C.H. Huang, Biomaterials 30 (2009) 5592–5600.
- [19] R.X. Yan, Y.D. Li, Adv. Funct. Mater. 15 (2005) 763.
- [20] X. Wang, Y.D. Li, Chem. Eur. J. 9 (2003) 5627.
- [21] X. Wang, Y.D. Li, Angew. Chem. Int. Ed. 42 (2003) 3497.
- [22] X. Wang, J. Zhuang, Q. Peng, Y.D. Li, Inorg. Chem. 45 (2006) 6661.
- [23] Z.L. Wang, Z.W. Quan, P.Y. Jia, C.K. Lin, Y. Luo, Y. Chen, J. Fang, W. Zhou, C.J. O'Connor, J. Lin, Chem. Mater. 18 (2006) 2030.
- [24] M. Wang, Q.L. Huang, J.M. Hong, X.T. Chen, Z.L. Xue, Cryst. Growth Des. 6 (2006) 1972.
- [25] M. Wang, Q.L. Huang, J.M. Hong, X.T. Chen, Z.L. Xue, Cryst. Growth Des. 6 (2006) 2169.
- [26] H. Lian, M. Zhang, J. Liu, Z. Ye, J. Yan, C. Shi, Chem. Phys. Lett. 395 (2004) 362.
- [27] H. Zhang, H.F. Li, D.Q. Li, S.L. Meng, J. Colloid Interface Sci. 302 (2006) 509.
- [28] J.L. Lemyre, A.M. Ritcey, Chem. Mater. 17 (2005) 3040.
- [29] H. Li, H.R. Li, Z.C. Guo, Y. Liu, Ultrason. Sonochem. 13 (2006) 359.
- [30] J.P. Ge, Y.D. Li, J. Mater. Chem. 13 (2003) 911.
- [31] L. Zhu, J.Y. Li, Q. Li, X.D. Liu, J. Meng, X.Q. Cao, Nanotechnology 18 (2007) 055604.
- [32] Z.J. Miao, Z.M. Liu, K.L. Ding, B.X. Han, S.D. Miao, G.M. An, Nanotechnology 18 (2007) 125605.
- [33] T. Xia, Q. Li, X.D. Liu, J. Meng, X.Q. Cao, J. Phys. Chem. B 110 (2006) 2006.
- [34] A. Fillankembo, S. Giorgio, I. Lisiecki, M.P. Pileni, J. Phys. Chem. B 107 (2003) 7492.
- [35] B. Wiley, Y.G. Sun, B. Mayers, Y.N. Xia, Chem. Eur. J. 11 (2005) 454.
- [36] Z.R. Tian, J.A. Voigt, J. Liu, B. Mckenzie, M.J. Mcdermott, J. Am. Chem. Soc. 124 (2002) 12954.
- [37] S.H. Im, Y.T. Lee, B. Wiley, Y.N. Xia, Angew. Chem. Int. Ed. 44 (2005) 2154.
- [38] D. Chen, K.B. Tang, F.Q. Li, H.G. Zheng, Cryst. Growth Des. 6 (2006) 247.
- [39] F. Tao, Z.J. Wang, L.Z. Yao, W.L. Cai, X.G. Li, Nanotechnology 17 (2006) 1079.
- [40] S. Nishibu, T. Nishio, S. Yonezawa, M. Takashima, J. Lumin. 126 (2007) 365.
- [41] G.X. Liu, G.Y. Hong, J.X. Wang, X.T. Dong, Nanotechnology 17 (2006) 3134.
- [42] L.E.B. Soledade, E. Longo, E.R. Leite, F.M. Pontes, F. Lanciotti, C.E.M. Campos, P.S. Pizani, J.A. Varela, Appl. Phys. A 75 (2002) 629.